BENDING EFFECT ANALYSIS OF METALLIC Z-PINS ON MODE I DELAMINATION TOUGHNESS OF DCB SPECIMEN

S.L. Zhong[1&], L. Tong[2]*
[1] Chengdu Aircraft Design and Research Institute, Sichuan Province, P.R. China, [2] School of Aerospace, Mechanical and Mechatronic Engineering, The University of Sydney, NSW 2006, Sydney, Australia
* Corresponding author (liyong.tong@sydney.edu.au)

Keywords: *delamination, toughness, z-pinning, DCB specimen*

1 Introduction

Composite materials have gained their acceptance among structural engineers during the last decades. In recent years, a substantial amount of airframe research has focused on developing advanced composites for use as heavily-loaded primary structures such as wing, fuselage and empennage components for both commercial and military aircraft [1].

Delamination is an important failure mode in laminated composite structures due to their low interlaminar fracture toughness. Through-thickness reinforcements, such as z-pinning, stitching, 3D weaving and braiding, can remarkably delay and/or resist delamination propagation in laminates [1-13]. Z-pinning technology has emerged in 1990s as a practical and cost-effective method in improving delamination resistance and already has shown a variety of potential applications in engineering structures.

According to Freitas et al [6], short z-pins can be carbon and glass fiber, titanium, stainless steel or aluminum etc. For fibrous pin at larger deflection, the fiber tow can be split in the form of micro cracks running parallel to the fibers within the pin. The strands formed by splitting slide relative to each other to accommodate large shear strain, which limits the magnitude of bending moment carried by the tow [7]. In contrast, metallic pins can have relatively higher bending resistance than fibrous ones. Therefore it is important to study the effect of bending moments reacted by a z-pin within crack bridging zone on crack growth resistance [11].

In this paper, a new discrete analytical model for metallic z-pin is presented to consider the traction loadings combining the axial force and bending moment of the z-pin. Geometrical and material nonlinearity of the z-pin model are taken into account in the bending moment calculation. The virtual crack closure technique (VCCT) is used to calculate mode I strain energy release rate (SERR) at the crack tip. Some numerical results are presented and discussed and shown to be in agreement with existing experimental and numerical results.

2 Basic Model and Concepts

Consider a DCB specimen reinforced with discrete z-pin rows as shown in Fig. 1. The total length, width and thickness of the DCB specimen are L, B and $2H$, respectively. Each row may have more than one z-pin dependent on the z-pin area density and the pitch distance d_p between the z-pin rows along the crack extension direction. The initial crack is created in the laminate mid-plane with length a_0. The distance of the initial crack tip to the first row of the z-pins is denoted by a_s. With an increase in the crack opening displacement δ and the induced external load P, the crack propagates along the mid-plane. When the delamination crack propagates into the z-pinned zone, the z-pins in the crack wake will exert the bridging traction loads and bending moments to limit the creation of delaminated crack surfaces. Thus a higher external load, compared to an un-pinned case, is developed in further crack propagation. Therefore z-pins can improve the delamination toughness of composite laminates.

The basic assumptions for developing the axial force-displacement relationship are similar to that presented by Jain and Mai [4] for independent through-thickness stitches. It is assumed that the z-pin is circular cylindrical and the bond between matrix and z-pin is completely frictional. The deformation in the matrix is assumed to be negligible. The frictional shear stress at the matrix-pin interface is also assumed to be a constant value. In this paper the effect of fiber abrasion or matrix crumbling during z-pin stretching, bending action and pull-out is neglected. No z-pin breakage occurs which is usually the case in mode I delamination of DCB specimen with small thickness and independent z-pinning reinforcements.

[&] This work was conducted during the period as a visiting scholar at the University of Sydney.

The Timoshenko beam theory is used to consider the effect of the shear deformation of the delaminated substrate. That assumes constant rotations of the cross sections for shear load with a shear deformation coefficient considered in the calculation of the shear deformation of the beam. When considering the shear deformation of the substrate at the crack tip, the zero slope of the substrate deflection curve, which is imposed in this study, will result in rotation of the cross section plane of the substrate at the crack tip.

A simple analytical z-pin model with the span from the centroid axis of the substrate to the assumed symmetrical delamination plane is developed in the derivation of the bending moment reactions of the z-pins to the substrate. The local elastic deformation in the matrix due to bending reaction of the z-pin is assumed to be negligible. In order to consider the elastic-plastic behavior of the metallic pin which may happen in bending action, a nonlinear stress-strain power law of the z-pin material is employed

3 Modeling of a Metallic Pin

3.1 Axial Forces-Displacement Relation of Z-Pin

The axial force-displacement relation for the pull-out of a single z-pin is based on frictional model [4]. The axial force in the z-pin can be written as

$$F = \tau \pi d_f \left[YU(\xi_1) + (H - S)(1 - U(\xi_1)U(\xi_2)) \right] \quad (1)$$

where

$$\xi_1 = 2\left[H - \frac{H}{r}\ln(1+r) \right](1+r) - \delta_f$$
$$\xi_2 = H - \delta_f \quad (2)$$

and τ is the frictional shear stress at the matrix-z-pin interface. d_f is the diameter of the z-pin, δ_f is the crack opening displacement at the z-pin location. $U(\xi_1)$ and $U(\xi_2)$ are the Heaviside step functions. The extensibility ratio r is defined as

$$r = \frac{\tau \pi d_f H}{A_f E_f} \quad (3)$$

where A_f and E_f are the cross-sectional area and the Young's modulus of the z-pin, respectively.

To consider the nonlinear behavior of bending moment of metallic z-pin, a simple non-linear material model is employed and the stress-strain law is represented by the Ludwick relation, i.e.

$$\sigma = \sigma_0 \varepsilon^{1/n} \quad (4)$$

where σ is the stress, ε is the permanent or elastic small strain at a point of a cross section of the beam, and σ_0 and n are given material constants which can usually be found in Ref. [14]. This relation applies primarily to metallic material of work harden type. The maximum extensibility ratio r for nonlinear elastic material of work harden type is given by

$$r = \frac{2}{n+1} \cdot \left(\frac{\tau \pi d_f H}{A_f \sigma_0} \right)^n \quad (5)$$

3.2 Analytical Beam Model of Z-Pin

Due to symmetrical assumption in Section 2, an analytical beam model between the crack plane at end A and the centroid of delaminated arm B at z-pin row location is provided to develop the traction force and bending moment of a single z-pin to the delaminated arm as shown in Fig. 2. The rotation at end B is denoted by ψ_r which is the rotation of the cross section of the delaminated arm at a z-pin row location. The rotation at end A is zero due to symmetry. The span of the z-pin model L_r is approximately the sum of deflection w_r and half the thickness of the delaminated arm.

The symmetrical constraining tensile force T and bending moment M_A are applied at end A. For equilibrium of the force system, the sum of the constraining forces at end A and B should be zero. The internal force T and bending moment M_B at end B are schematically shown in Fig. 2. Neglecting the uneven pressure at the interface of the matrix-z-pin due to rotation ψ_r in obtaining the axial force F of the z-pin in Section 3.1, the resultant force T at end B can be considered as the sum of the axial force F and the uneven normal pressure acting on the z-pin cylinder, i.e. $T = F/\cos\psi_r$. From Fig. 2, the bending moment at a location x on the central axial of the beam is

$$M(x) = M_B + T(y - \delta_v) \quad (6)$$

For a uniform circular cross-section Bernoulli-Euler beam of non-linear elastic Ludwick type materials, assuming that the average axial tensile strain is small compared to the maximum bending strain, the nonlinear differential equation for the deflection of the z-pin beam model is given as follows:

$$\frac{y''}{(1+y'^2)^{3/2}} = \frac{M^n}{K_n} \quad (7)$$

where $K_n = \sigma_0^n I_f^n$, and I_f can be obtained by

$$I_f = \frac{2\beta n}{3n+1}\left(\frac{d_f}{2} \right)^{(3n+1)/n} \quad (8)$$

and d_f is the diameter of the z-pin, coefficient β can be determined by the following integral:

$$\beta = \int_0^{\pi} (\sin\theta)^{\frac{n+1}{n}} d\theta \quad (9)$$

The boundary conditions of Eq. (7) are as follows:

$$\begin{cases} y(0) = 0 \\ y'(0) = 0 \\ y'(L_r - \delta_h) = \tan\psi_r \end{cases} \quad (10)$$

Similar to solving the differential equation of the delaminated arm, the numerical integration of Eq. (7) is conducted by using the fourth order Runge-Kutta method with the first two initial conditions in Eq. (10). There are two controlling unknown parameters in Eq. (7), i.e. M_B and δ_v. Again the shooting method [15] is employed in two procedures: one is for an assumed M_B, determining the deflection δ_v at end B; the other is determining the required bending moment M_B, which results in the prescribed rotation ψ_r at end B.

In the above derivation, the bending moment was obtained for metal materials of the Ludwick type. For a linear elastic material, i.e., $n = 1$ and $\sigma_0 = E_f$, the bending moment M_B for small deformation, which means $1 + y'^2 \approx 1$, can be solved in a closed-form solution as follows:

$$M_B = \frac{E_f I_f \psi_r \sqrt{\gamma}(e^{\sqrt{\gamma}L_r} + e^{-\sqrt{\gamma}L_r})}{e^{\sqrt{\gamma}L_r} - e^{-\sqrt{\gamma}L_r}} \quad (11)$$

where $\gamma = \dfrac{T}{E_f I_f}$.

It is worth pointing out that the bending moment M_B on the z-pin for linear elastic material constants may become so large that the bending stress on the beam is beyond the ultimate tensile strength of the material. In fact, bending stresses on ductile pin exceed the yield limit and plastic bending occurs. Consider an extreme case: for a z-pin of circular cross section with diameter d_f, an ultimate condition of plastic bending, namely the plastic hinge, is reached, and the limit plastic bending moment is

$$M_{\max} = \sigma_{tu} d_f^3 / 6 \quad (12)$$

where σ_{tu} is the ultimate tensile strength of the material.

After obtaining the resultant force T and bending moment M_B at end B for a single z-pin, the bridging load and moment of a z-pin row (with m z-pins) to the delaminated arm are given by

$$\begin{cases} T_r = mT \\ M_r = mM_B \end{cases} \quad (13)$$

4 Formulation of Strain Energy Release Rate

For unidirectional DCB specimen mode I delamination test, G_I can be considered as the total strain energy release rate. The SERR G_I at the crack tip is calculated using the virtual crack closure technique (VCCT) and employed as the fracture toughness of the DCB specimen mode I delamination. This method is based on Irwin's contention that if a crack extends by a small amount Δa, the energy absorbed in the process is equal to the work required to close the crack to its original length.

For a crack length a, the constraint shear force and moment at the crack tip are Q_0^a and M_0^a, respectively, the rotation of the cross section of the substrate at the crack tip is ψ_0^a. Assuming a virtual crack extension Δa, the deflection w_Δ^V and the rotation of the cross section ψ_Δ^V of the substrate at the original position of the crack tip can be obtained. The constraint shear force and moment at the virtual crack tip are Q_0^V and M_0^V, respectively, the rotation of the cross section of the substrate at the virtual crack tip is ψ_0^V. The strain energy release rate G_I at the crack tip can be calculated as follows:

$$G_I = \frac{M_0^a \psi_\Delta^V - M_0^V \psi_0^V - Q_0^a w_\Delta^V}{B\Delta a} \quad (14)$$

To obtain the critical strain energy release rate, due to z-pinning, G_{IR}, the applied loading conditions corresponding to the intrinsic unpinned critical strain energy release rate G_{IC} at the crack tip should firstly be iteratively searched. Then by removing all the z-pinning traction loads and moments, the strain energy release rate can be re-calculated by the same geometry and applied loading conditions, and this new value of strain energy release rate is G_{IR}.

5 Results and Discussion

5.1 Load-Displacement Curve of Unpinned DCB

Consider a z-pin reinforced DCB specimen with initial crack length a_0=50mm, the total thickness of DCB $2H$=3mm and the width B=20mm. The DCB is made of unidirectional (UD) IMS/924 carbon/epoxy composite [8-10,13], and the elastic properties for the DCB specimen are: E_{11} = 143 GPa (unpinned specimen), G_{12} = 4.4 GPa.

The critical strain energy release rate G_{IC} can be obtained from the experimental data of unpinned DCB specimen delamination test. Due to uncertainties such as the exact initial crack length, the initial shape of crack front, resin rich or resin starved condition at the initial crack tip, etc., the load and the corresponding crack opening

displacement at the beginning of the crack extension may not be reliable to calculate G_{IC} accurately. The load-deflection experimental data during stable crack growth can be used to calibrate G_{IC} value for given material constants and geometrical properties of the DCB specimen. An approximate G_{IC} value of 270 J/m^2 can be obtained based on fracture mechanics. The load-displacement experimental data of an unpinned DCB specimen test and the numerical results together with two variations of G_{IC} are shown in Fig. 3. The critical strain energy release rate G_{IC} = 270 J/m^2 was used for z-pin reinforced UD IMS/924 DCB specimen mode I delamination at the crack-tip zone.

Tensile tests [13] on z-pin of diameter 0.51mm made from titanium or T300/BMI revealed that the titanium pins had a yield stress of 1100 MPa and an ultimate tensile strength of 1230 MPa. The T300/BMI pins are linear elastic till failure strength of 1200 MPa. For UD composite substrate, the frictional shear stress τ is 15 MPa for titanium pins and 19 MPa for T300/BMI fibrous pins. The material modulus [16] for T300/BMI pin is E_f =138.6 GPa. The material properties of the titanium pin are: Young's modulus E_f =105 GPa, equivalent material constants of work harden type σ_0 = 2737 MPa, n = 5.0 according to tensile tests data and Ref. [17]. Assuming the material properties and the frictional shear stresses in pin-matrix interface for different diameters are the same as the experiment results [13].

5.2 Comparison of P-δ and G_{IR}-a Curves with Bending Effect of Titanium Z-Pins

To analyze the bending effect of z-pin with different sets of material constants which contribute to the delamination resistance of z-pinned DCB specimen test, consider titanium z-pinning reinforcements in a UD IMS/924 DCB specimen mode I delamination test [8-10,13]. The geometrical parameters and material properties of a DCB are given in section 5.1. The distance of the initial crack tip to the first row of the z-pins is 1 mm. The diameters of z-pin considered are 0.28 mm and 0.51 mm. The z-pin area densities of 0.5%, 1% and 2% are studied. The bending effect of the z-pins on P-δ and G_{IR}-a curves based on both the work harden material constants and linear material constants with fully plastic bending moment shows an increase in load P and G_{IR} values. This study shows that the diameter of the z-pin, which is directly related to the capacity of the bending resistance of the z-pin, is the predominant factor in the bending effect of the z-pin. The larger the diameter of the z-pins, the more increase in bending effect on delamination resistance. Higher z-pin densities show moderate increase in delamination toughness representing that a greater proportion of plastic bending behavior of the z-pin is developed. An average increase of approximate 3-4%, 7-10% in load P and G_{IR} values after the full development of the crack bridging zone are observed for the z-pin diameter of 0.28 mm and 0.51 mm, respectively. Numerical results of the bending effects on the P-δ and G_{IR}-a curves of the DCB specimen for z-pin diameter of 0.28 mm, 0.51mm with area density of 1% are shown in Fig. 4 and Fig. 5, respectively.

5.3 Comparison with Experimental Data and Some Preceding Results

Consider a mode I delamination test of a UD IMS/924 DCB specimen reinforced with T300/BMI z-pins with a diameter of 0.28 mm and an area density of 0.5% in [9]. The initial crack length is 50mm. The z-pins are distributed within a band of 25 mm in length starting at about 1.5 mm beyond the initial crack tip adapted according to crack length curves in [9]. The experimental data and numerical results of the force-displacement curves together with the FE results in [8] are shown in Fig. 6 where the abscissa is half the crack opening displacement δ as defined in this paper. The FE result in [8] was obtained by using shell element modeling the composite laminate with transverse shear deformations. The critical loads for initial delamination propagation calculated are almost the same as the experiment result, about 40 N as indicated by the first sudden drop of the load. The "stick-slip" behavior of the load-displacement curves is the typical phenomenon for the presence of a new z-pin row and is more apparent for smaller z-pin densities. The maximum load of about 80 N is observed in the region at about the displacement of 8 mm to 10 mm for all curves in Fig.6. The analytical results from these two modeling methods are reasonable and agreeable to the experimental data except for minor discrepancies possibly because of the indeterminate factors in the experiment and different modeling methods of the specimen.

The delamination resistance curve calculated using VCCT in this study is shown in Fig. 7 together with two other curves taken from [9], which were obtained from the corrected beam theory and the adapted data analysis method, respectively, on the basis of experimental compliance data results using some correction factors and modifications of axial

modulus and G_{IC} for the specimen, and another curve of FEA results taken from [10]. Both the pattern and magnitude of the G_{IR}–a curve calculated using the present approach are reasonable and consistent with these previous results.

It is interesting to note that the present analytical results are in good agreement with the FEA results [10] except for minor difference after reaching saturation of the crack bridging zone which is in part due to the consideration of bending effect of the z-pins.

7. Conclusion

In this paper, a new simple analytical beam model is proposed to consider the bending effect of z-pins on mode I delamination toughness of DCB specimen. The geometrical and material nonlinearities and loading conditions of the z-pin model are employed to take into account the interaction of the bending moment and axial load. The numerical analyses of a DCB specimen reinforced with titanium z-pins reveal favorable contributions of the bending effect of the z-pins to the delamination toughness of DCB specimens. The load-displacement curve and G_{IR}-crack length curve of a DCB specimen based on the analytical beam models of the substrate and the z-pins proposed in this study are calculated and validated against the available experimental and numerical results.

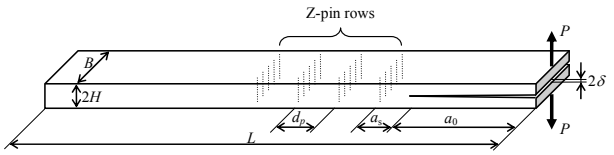

Fig.1. Schematic representation of a z-pinned DCB specimen test

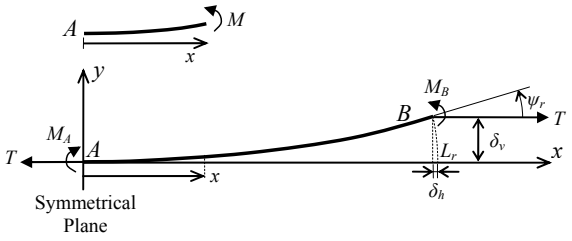

Fig.2. Nonlinear analytical beam model for a single z-pin

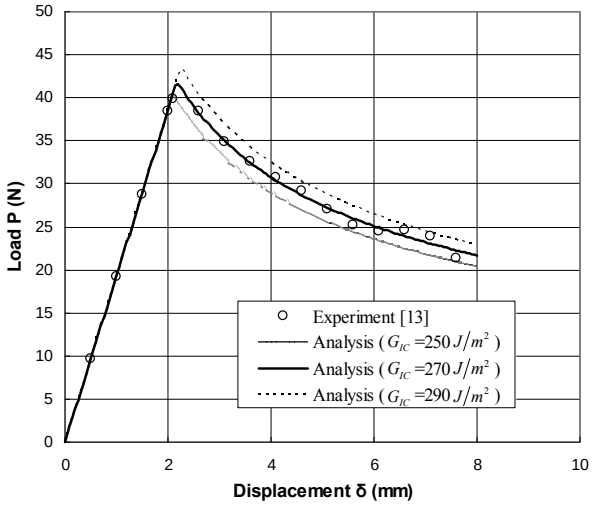

Fig.3. Load-displacement curves for unpinned DCB specimen

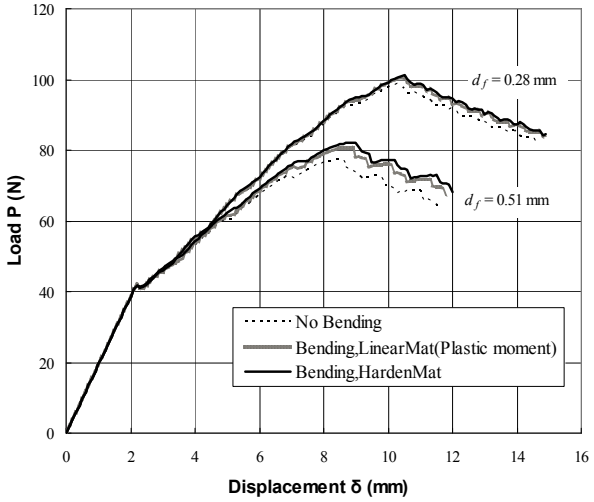

Fig.4. Influence of bending effect of z-pins on load-displacement curves

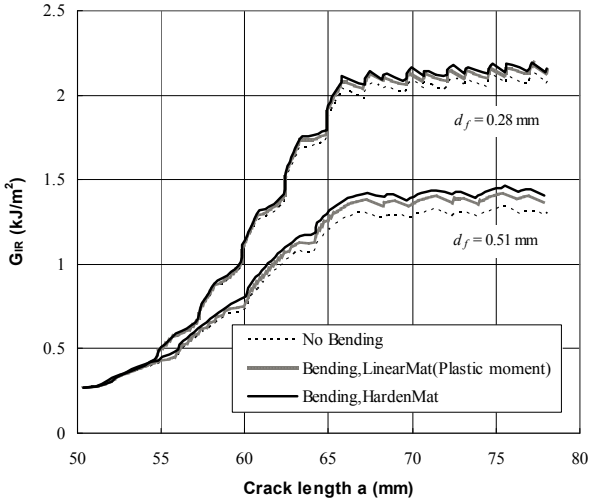

Fig.5. Influence of bending effect of z-pins on G_{IR}-crack length curves

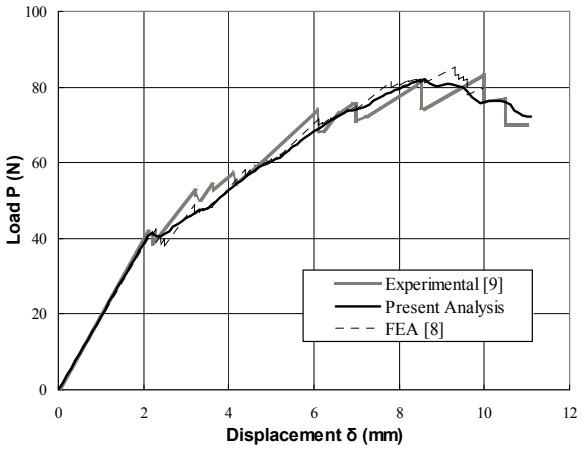

Fig.6. Comparison of load-displacement curves from experimental and numerical results

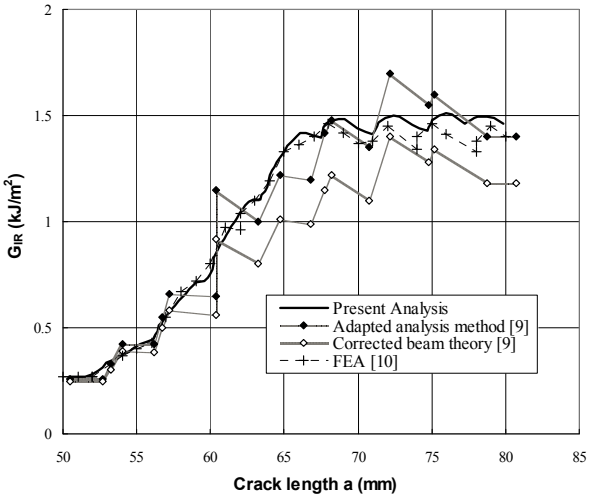

Fig.7. Mode I delamination resistance curves for a DCB specimen

Acknowledgement

The authors are grateful to the support of the China Scholarship Council to S.L. Zhong during his affiliation with The University of Sydney as a visiting scholar.

References

[1] M. C-Y Niu "*Composite Airframe Structures*". Hong Kong Conmilit Press Ltd., 2000.

[2] L. Tong, A.P. Mouritz, and M.K. Bannister "*3D Fibre Reinforced Polymer Composites*". Elsevier Science Ltd., 2002.

[3] K. Dransfield, C. Baillie, and Y.-W. Mai "Improving the Delamination Resistance of CFRP by Stitching - A Review". *Composites Science and Technology*, 50: pp 305-317, 1994.

[4] L. K. Jain and Y.-W. Mai "On the Effect of Stitching on Mode I Delamination Toughness of Laminated Composites". *Composites Science and Technology*, 51: pp 331-345, 1994.

[5] A.P. Mouritz, K.H. Leong, and I. Herszberg "A Review of the Effects of Stitching on the In-plane Mechanical Properties of Fibre-reinforced Polymer Composites". *Composites A*, 28A: pp 979-991, 1997.

[6] G. Freitas, C. Magee, P. Dardzinski, and T. Fusco "Fiber Insertion Process for Improved Damage Tolerance in Aircraft Laminates". *Journal of Advanced Materials*, 25: pp 36-43, 1994.

[7] B. N. Cox "Constitutive Model for a Fiber Tow Bridging a Delamination Crack". *Mechanics of Composite Materials and Structures*, 6: pp 117-138, 1999.

[8] M. Grassi, X. Zhang "Finite Element Analyses of Mode I Interlaminar Delamination in Z-fibre Reinforced Composite Laminates". *Composites Science and Technology*, 63: pp 1815-1832, 2003.

[9] I.K. Partridge, D.D.R. Cartié "Delamination Resistant Laminates by Z-fiber Pinning: Part I Manufacture and Fracture Performance". *Composites A*, 36: pp 55-64, 2005.

[10] D.D.R. Cartié, M. Troulis, I. K. Partridge "Delamination of Z-pinned Carbon Fibre Reinforced Laminates". *Composites Science and Technology*, 66: pp 855-861, 2006.

[11] L. Tong and X. Sun "Bending Effect of Through-thickness Reinforcement Rods on Mode I Delamination Toughness of DCB Specimen I: Linear Elastic and Rigid-perfectly Plastic Models". *International Journal of Solids and Structures*, 41: pp 6831-6852, 2004.

[12] W. Yan, H.-Y. Liu, Y.-W. Mai "Numerical Study on the Mode I Delamination Toughness of Z-pinned Laminates". *Composites Science and Technology*, 63: pp 1481-1493, 2003.

[13] D.D.R. Cartié, B.N. Cox, N.A. Fleck "Mechanisms of Crack Bridging by Composite and Metallic Rods". *Composites A*, 35: pp 1325-1336, 2004.

[14] Datsko, Joseph "*Material Properties and Manufacturing Processes*". New York, Wiley, 1966.

[15] K. Lee "Large deflections of cantilever beams of non-linear elastic material under a combined loading". *International Journal of Non-Linear Mechanics*, 37: pp 439-443, 2002.

[16] P. K. Mallick "Laminated Polymer Matrix Composites" *Composites Engineering Handbook*, Marcel Decker, 1997.

[17] Datsko, Joseph "*Material Properties and Manufacturing Processes*". New York, Wiley, 1966.